

Using PXRD to Investigate the Crystallization of Highly Concentrated Emulsions of NH_4NO_3

E.E. Ferg^{1,*} and I. Masalova²

^aDepartment of Chemistry, Nelson Mandela Metropolitan University, P.O. Box 77000, Port Elizabeth 6031, South Africa.

^bDepartment of Civil Engineering, Cape Peninsula University of Technology, P.O. Box 652, Cape Town 8000, South Africa.

Received 24 December 2009, revised 19 October 2010, accepted 22 December 2010.

ABSTRACT

The process of crystallization of highly concentrated emulsions of ammonium nitrate can be studied using powder X-ray diffraction. The dispersed particles comprise a supercooled aqueous solution of the ammonium nitrate salt and are dispersed in a paraffin-based oil. This results in a thermodynamically unstable system that 'ages' with time resulting in changes in rheological properties and its phase composition where the collapse of the supercooled aqueous solution forms the crystallized salt. The crystallization processes of these emulsions are kinetically slow and can take up to a few months to crystallize completely. The general approach to this type of analysis is to determine the change in crystalline diffraction peak intensities relative to the halo due to the amorphous content. However, there are a number of problems associated with this method which are addressed by using Rietveld refinement methods which can take into account factors such as preferred orientation, crystallite size variations and mixtures of solid phases. The study showed that the ammonium nitrate emulsions kept at room temperature slowly crystallize predominantly to the room temperature solid ammonium nitrate phase IV. However, depending on the formulations used some samples showed crystallization to the high temperature ammonium nitrate phase II before changing to phase IV. The crystallization change could be modelled by the well-known JMAK kinetic relationship.

KEYWORDS

Ammonium nitrate emulsion, crystallinity, X-ray diffraction.

1. Introduction

Highly concentrated emulsions (HCE) are used in a variety of applications that can range from cosmetics, food industry to 'liquid explosives'.^{1,2} In particular, the flow or rheological properties of liquid explosives are well described and are of practical importance in their application in open-cast mining.^{3,4} The dispersed particles comprise a supercooled aqueous solution of the ammonium nitrate (AN) salt dispersed in a paraffin-based dispersant that results in a thermodynamically unstable system. Hence, the system 'ages' with time, resulting in changes in rheological properties and phase composition. This is seen by the collapse of the supercooled aqueous condition to form the crystallized salt. The crystallization of solutions of supercooled phases are in most cases sporadic and quick, where small nucleation sites within the system would cause the entire system to change over very short periods of time. However, the crystallization processes of emulsions of the supercooled salts are kinetically slow and can take up to a few months to crystallize completely. The instability of the emulsion results in the rupture of the droplets that in some cases can encourage further nucleation and crystallization of adjacent droplets. The droplets within these emulsions usually contain a range of additives and surfactants that stabilize the colloidal two-phase system by preventing contact between the dispersed droplets.

The emulsions are usually made by the addition of a hot (80 °C) supersaturated aqueous solution of AN (that contains small amounts of salts of other elements such as calcium or sodium) to an organic phase such as liquid paraffin. The dispersed phase of the emulsions consists of droplets of the supercooled concentrated solution where the water content is less than 20 %

by mass at room temperature. The continuous phase is a solution of an emulsifier that contains about 15 % of various hydrocarbon oils and a range of surfactants that would influence the stability of the emulsion.

The resultant emulsion is obtained with finely dispersed droplets within an oil matrix where kinetic stability is usually achieved by the addition of surfactants and other stabilizers. Studies have shown that depending on the formulation and ratio of the various components, the crystallization of the emulsion can vary significantly with time.³ The degree of crystallization of the emulsion has a significant influence on a number of rheological properties such as the ability to transport and pump the material to its application and on its subsequent detonation ability.⁵ The degree of crystallization can be measured in part by calorimetric methods or by using polarized optical microscopy. These methods are, however, limited due to the sample size used and are not necessarily representative of the larger sample matrix. Villamagna and Whitehead described the use of ¹⁴N NMR spectroscopy to determine the degree of crystallization of ammonium nitrate emulsions.⁵ By using suitable standard solutions, they were able to measure the amount of nitrate ions that remained in the supersaturated emulsion droplets when compared with the crystallized nitrate salt using the ¹⁴N NMR signal. However, little or no information about the actual crystallized phase could be determined from these techniques.

Powder X-ray diffraction (PXRD) has found application in the field of pharmaceutical and polymer materials analysis to determine the relative amounts of crystalline to amorphous content of solid materials where their degree of crystallinity is determined and studied.^{6–10} These materials often comprise a single chemical compound that exists as both the amorphous and crystalline

* To whom correspondence should be addressed. E-mail: ernst.ferg@nmmu.ac.za

phases in synthesized mixtures. Some of these pharmaceutical mixtures can show changes in their crystallinity with time and PXRD was successfully used to study their crystallization rates.⁸ The general approach to the analysis is the determination of the change in crystalline diffraction intensities relative to the scattering due to the amorphous content. Some recent literature articles describe the determination of the degree of crystallinity of a sample using Rietveld refinement of the entire diffraction pattern of a semi-crystalline sample.¹⁰ Rietveld whole pattern refinement is extensively used in the quantification of often complex solid mixtures such as cements that makes use of the crystal structural information of the phases present in the mixture. Modern commercial software provides ease of use and can also take many sample and instrumentation factors into consideration such as preferred orientation, crystallite sizes, sample displacement, absorption factors and the contribution due to amorphous material.^{11–14}

It is important that a clear distinction is made between the concept of the degree of crystallinity or relative crystallinity of a material to that of the crystallization or crystallization rate that occurs over a period of time. The crystallinity of a solid material is usually specified as a percentage of the mass or volume of the material that is crystalline when compared with the rest of the amorphous matrix. Even within a material that is considered as completely crystalline there are degrees of structural imperfections that can vary, thereby creating independent crystalline regions (grains or crystallites) with various orientations. These and other defects can reduce the degree of structural perfection and thereby influence the degree of crystallinity measured. Material structural studies using PXRD would consider the average diffraction pattern of a powdered material with all its imperfections and regions of reduced crystallinity. Typical examples are polymer materials that show considerable variation in their crystalline regions where there are some relatively large molecular mass regions that have long-range order with interspersed well-defined highly ordered crystalline regions. The absolute crystallinity of a sample is usually determined by the addition of a suitable standard material such as amorphous silica to a matrix that contains a similar unknown amount of the amorphous material, or by the careful preparation of a number of standard samples that contain known amounts of the crystalline and amorphous materials. In many cases, where this is not possible, only relative crystallinity can be determined, where the ratio of some criteria for a fully crystalline and a fully amorphous sample are then compared.

On the other hand, crystallization could be defined as a process that occurs over a period of time. These processes of crystal growth within a non-crystalline matrix such as a supersaturated salt solution or in a pharmacologically active material usually originates at a nucleating region that spreads, over a period of time, to the rest of the material.⁸ Hence, by measuring the change in the amount of crystalline material relative to that of the remaining amorphous sample, the crystallization rate can be determined, provided that it is slow enough to allow for multiple PXRD analyses of the same sample to be done over time.

The five solid phases of pure ammonium nitrate (AN) and their transition temperatures have been extensively studied.^{15–17} The space groups, crystal systems and approximate transition temperatures of the five phases are summarized in Table 1.

In the study of AN emulsions at room temperature, the solid phase IV is of primary interest. As the supercooled solution starts to crystallize with time, PXRD is an ideal method for determining the amount of crystallites present relative to the rest of the

Table 1 The space groups and transition temperatures of the five solid phases of AN.¹⁸

Phase	Transition temperature/°C	Space group (crystal system)
I	above 125	<i>Pm3m</i> (cubic)
II ^a	84	<i>P42₁m</i> (tetragonal)
III	32	<i>Pnma</i> (orthorhombic)
IV ^a	–17	<i>Pmmm</i> (orthorhombic)
V	below –17	<i>Pccn</i> (orthorhombic)

^aNote: If the moisture content of the material is below 23 %, phase IV can transform directly to phase II at 51 °C.¹⁵

amorphous emulsion. This article describes the methodology of determining the relative amounts of the crystallized dispersed phase of AN in the emulsion matrix over time. The difficulty of sample preparation and the use of various data analysis methods will also be discussed. The technique was then applied to typical AN emulsion samples that would be considered to have a relatively short period of stability, showing the usefulness of the PXRD technique to describe relative crystallization rates. The influence of varying the formulations of the emulsion and their preparative techniques on both the crystallization and rheological properties are reported elsewhere.^{3,19}

In addition, the X-ray diffraction patterns of partially crystallized and fully crystallized samples are investigated at different temperatures and compared with results obtained by calorimetric analytical methods. It is well known that pure AN undergoes a range of solid phase transitions under various conditions of humidity and temperature.¹⁵ The phase transitions that are near room temperature might influence the properties of the emulsions that would be exposed to a range of temperature fluctuations during manufacturing, transportation and applications.

2. Experimental

For the purpose of this study, the following samples were prepared that can be considered to have relatively short crystallization times: 20 and 35 % by mass, respectively of SMO (sorbitan mono-oleate) were added to a hydrocarbon oil known as Mosspar[®]. Hot solutions of about 80 % AN were added to the hydrocarbon oil mixture at a mixing rate of 60 rev min^{–1} for 2 min. After this, the emulsion was mixed at high speed (255 rev min^{–1}). The resulting emulsions were cooled to room temperature and the average droplet size was determined by laser diffraction on a Mastersizer-2000 (Malvern Instruments Ltd., Malvern, Worcs., UK) to be approximately 10 μm. For comparison purposes, a third AN emulsion was prepared that was considered to have longer crystallization times. The sample contained 20 % PIBSA (poly(isobutylene succinic) anhydride) in Mosspar[®] that was prepared with a final mixing rate of 255 rev min^{–1} resulting in an average droplet size of 15 μm.

X-ray diffraction analysis was done on a Bruker D8 powder diffractometer (Karlsruhe, Germany) using Cu radiation. Conventional Bragg Brentano geometry was used with a Ni filter at the detector, a 2θ scan range of 10 to 60 ° at 0.02 ° step intervals and at a scan rate of 1 step s^{–1}. For the duration of the crystallization study, the samples were kept at 22 °C in a closed container to prevent possible moisture loss, and only small amounts removed for PXRD analysis. The emulsion samples were placed in a standard top-loading polycarbonate sample holder and supported on a horizontal rotating sample stage. Standard sample preparation techniques were used to fill the emulsion sample into the sample holder ensuring that the surface was level with the top of the holder. A glass slide was

used for this purpose, which would often introduce preferred orientation of the crystallites near the surface of the sample. This, however, could not be avoided due to the nature of the sample, and the preferred orientation factor was then taken into consideration during the data analysis and refinement procedure. The crystal structural information of the various AN phases were obtained from the ICDD data base and the degree of crystallinity was determined by using the Topas 3.0 software (Karlsruhe, Germany).^{18,20}

Variable temperature powder X-ray (VTPXRD) studies of the emulsion samples were done by placing a small amount of the required sample on a modified heating stage and allowing the sample to heat slowly at a rate of 1 °C min⁻¹ to a preset temperature. An X-ray transparent 7.5 μm Kapton film was used to seal the sample and holder in order to prevent any loss of moisture during the heating steps. The scan angles and instrumental settings were the same as for the room temperature study. The sample was allowed to heat to the specified temperature, allowing it to equilibrate for 30 min before X-ray scan analysis. The temperatures used in the study were 40, 50 and 60 °C. Differential scanning calorimetric measurements were done on a Mettler DSC820 (Mettler-Toledo, Inc., Columbus, OH, USA). The samples of interest were sealed into an Al DSC pan and heated to 60 °C at a rate of 0.5 °C min⁻¹.

3. Results and Discussion

3.1. Determining the Crystallinity of AN Emulsions

A number of authors describe the principle of measuring crystallinity of semi-crystalline materials such as polymers and pharmaceuticals.^{6–9} The principle relies on the fact that, if the incident X-ray intensity is constant, the total intensity of the diffracted scattering of a body of fixed mass should be constant, irrespective of the structure of the atoms in the bulk of the body. This implies that the diffracted intensity should remain constant, irrespective of the ratios of crystalline to amorphous regions in the scattered body. If the composition of the crystalline region and the amorphous regions are clearly distinguishable and if the interferences between the scatterings of the two regions can be ignored, the total scattering can be divided into the crystalline scattered (I_{cr}) region and the amorphous scattered (I_{am}) region. The degree of crystallinity (X_{cr}) can be defined by the respective masses of the crystalline (M_{cr}) and amorphous (M_{am}) regions as:

$$X_{cr} = \frac{M_{cr}}{(M_{cr} + M_{am})} \quad (1)$$

The ratios of the scattering densities of the X-rays from the amorphous and crystalline regions of a material are nearly equal to the ratio of the masses of the two types of regions as long as the compositions of the two regions are similar. Hence, the crystallinity of the material can be determined from the ratio of the total scattering intensities of the two regions.

This relationship can then be used to find the relative crystallinity of a sample material that has some amorphous content with respect to a reference material that exhibits a high degree of crystallinity. According to Kakudo and Kasai, the diffraction intensity of the material with an unknown crystallinity (I_u) would be measured and compared with the corresponding intensities of the peaks (I_{cr}) of the highly crystalline material and that of the halo (I_{am}) obtained from the completely amorphous sample.⁷ The degree of crystallinity (X_{cr}) can be determined by

$$X_{cr} = \frac{(I_u - I_{am})_j - K}{(I_{cr} - I_{am})_j} \quad (2)$$

where the intensity differences ($I_u - I_{am}$)_j and ($I_{cr} - I_{am}$)_j are determined at different specific 2θ diffraction angles (j). The results are plotted on a graph of ($I_u - I_{am}$)_j versus ($I_{cr} - I_{am}$)_j where the slope of the straight line is then the crystallinity (X_{cr}). If the scales of the various diffraction intensities are well matched and approach the origin, the y-intercept (K) is zero.

This principle can be used to determine the relative crystallinity from the intensity differences of the fully crystallized and completely amorphous phases of the room-temperature AN emulsion. This was done by considering the fresh supercooled emulsion as almost completely amorphous (I_{am}). The fully crystalline phase (I_{cr}) was observed when the AN emulsion had broken down, resulting in nearly complete crystallization of the material. This was achieved by observing the fact that a selected sample indicated very little or no change in their respective diffraction peak intensities in the diffraction pattern with time (over a few weeks). The results in Fig. 1 show the typical variation in the diffraction pattern and peak intensities of an emulsion with time. In most samples, the crystalline phase at room temperature would correspond to phase IV of AN, where the first eleven peak positions corresponded to the diffraction pattern obtained from the reference data base.¹⁸ Peaks with reasonable intensities for 2θ between 5 and 60 ° were then chosen for the study.

The intensities for the amorphous halo (I_{am}) with the same eleven 2θ peak positions as that of the crystalline phase were taken from a sample that had shown no crystalline peaks. The intensities of the fully crystalline (I_{cr}) material were taken of an AN sample 23 weeks after manufacturing. The crystalline patterns of the sample showed no further increases in their relative intensities when compared with the results of the preceding week. Hence, the emulsion can be considered as having fully crystallized. A sample of unknown crystallinity that was analysed before obtaining the fully crystallized sample can then be analyzed for its relative crystallinity by considering the differences of ($I_u - I_{am}$) and ($I_{cr} - I_{am}$) as shown graphically in Fig. 2.

This difference can be determined for all eleven reference peaks selected and then plotting ($I_u - I_{am}$) versus ($I_{cr} - I_{am}$). The resulting straight line would pass through the origin and the slope would give an indication of the relative crystallinity of the unknown sample (Fig. 3). In this example the relative crystallinity of the unknown sample would be 73 % with a relatively good R² correlation factor.

However, by considering only the peak intensities, considerable error can be introduced since the calculations do not consider factors such as sample displacement, sample absorption, instrumental error, crystallite size variation that influences the peak broadening, and especially preferred orientation. This was found to be particularly true in samples with low crystallinity where poor correlation factors were obtained (Fig. 4).

PXRD full-pattern analysis has improved considerably over the years by using Rietveld refinement techniques that are incorporated into 'user-friendly' software. The method considers the entire diffraction pattern in its calculations, allowing one to solve relatively complex crystal structures and to quantify multi-component samples such as cements and clays.²¹ Commercial software such as Topas[®] makes use of the fundamental instrumental parameter approach and the crystal structural characteristics of the material phases under investigation.²⁰ With these methods, the refinement approach used the crystalline structural parameters of the observed AN phase obtained from literature and compared it with predefined peaks that contribute to the amorphous halo of a newly made emulsion sample.

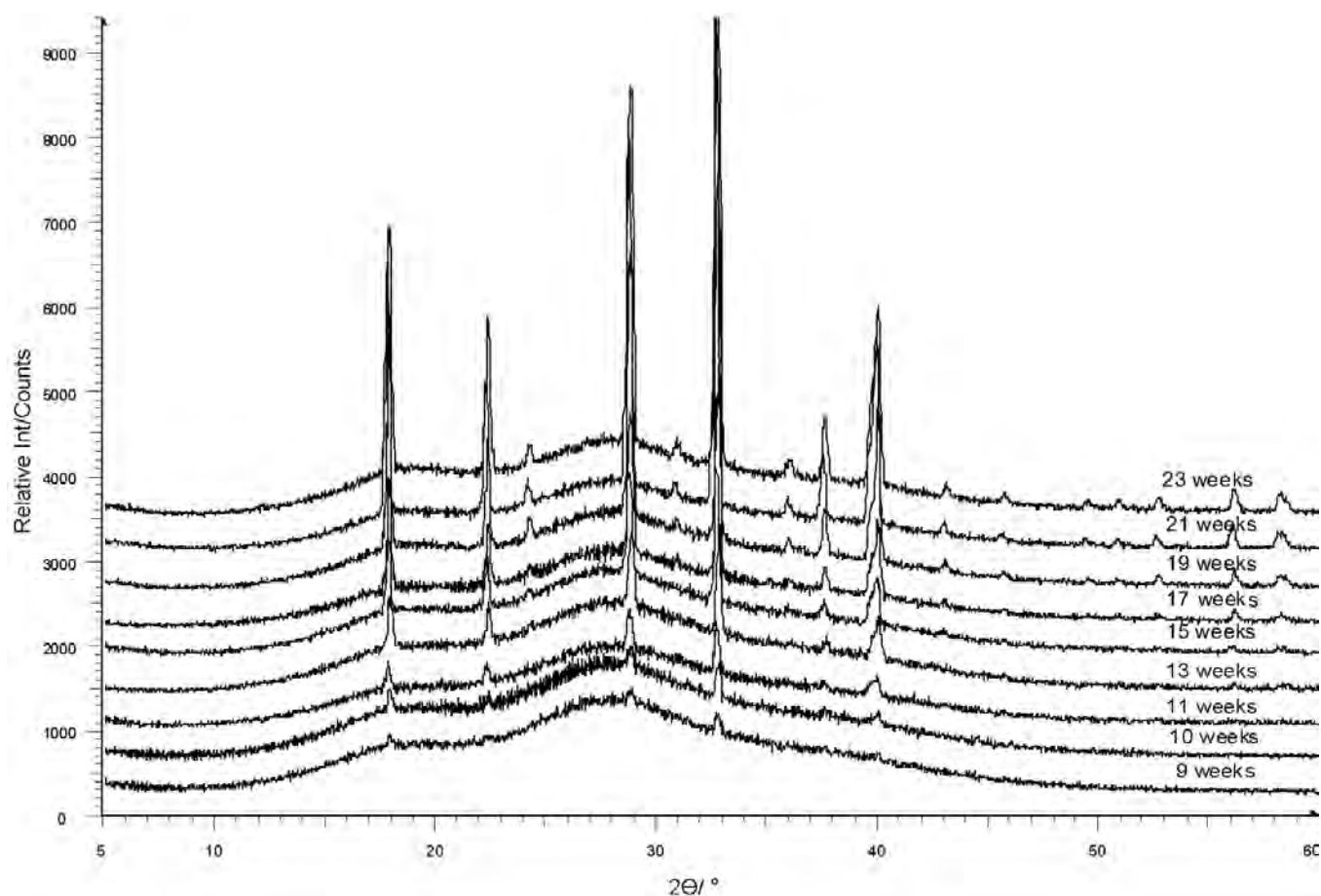


Figure 1 Staggered X-ray diffraction patterns of an AN emulsion sample made with 35 % SMO analyzed over a few weeks showing the increase in diffraction peak intensity of the AN phase IV.

This was done by firstly refining the shape of the amorphous halo scattering with suitable peak profiles that described the shape of the amorphous character (Fig. 5).

In this case the scattering halo due to the amorphous sample was described by three simple symmetric Gaussian peaks with a suitable low-order polynomial equation for the background. The peak positions of the amorphous halo were kept fixed during further analysis of the partially crystalline samples, assuming that the drift in the peak positions between samples would be negligible that could arise due to slight variations in the emulsion droplet size. Hence, only the peak areas were allowed to refine for the contribution of the amorphous halo to the rest of the crystalline material. Any subsequent analysis of 'aged' emulsions that showed crystallization of the AN with time was done by refining the contribution of the crystalline AN phase IV relative to the amorphous phase. For example, the refinement results of a 'fully aged' emulsion sample showed the degree of crystallinity to be 21.7 % (Fig. 6). The weighted residual (Rwp) was 9.36 and the goodness of fit (GoF) was 1.24.

In the analysis, factors such as preferred orientation were easily taken into consideration where the (110) and (111) peaks for the AN phase IV were shown to have very strong preferred orientation in some samples. The software would subsequently refine the respective peaks with a preferred orientation factor. The preferred orientation of the crystallites occurred during sample preparation where it was difficult to ensure random distribution of the crystallites in the uniformly filled top loading sample holder.

Noticeably, the results are reported as relative crystallinity that was determined by the software. In order to determine accurate

absolute crystallinity of the crystallized samples, one would have to either use the internal standard or standard addition methods to add a known amount of a suitable reference material to the sample. The reference material would have to have similar material characteristics to those of the bulk sample and have no influence on the crystallization process. In this case, it would also be difficult to obtain a homogenous mixture with the AN emulsions, without any chemical influence on the properties of crystallization. Villamagna and Whitehead reported similar problems of preparing samples for ^{14}N NMR spectroscopy by adding a suitable standard material to an emulsion sample.⁵ By repeating the analysis of the fully aged sample over a few weeks and observing little or no change in the degree of crystallinity, one could then consider the sample as having fully crystallized and deduce that 100 % of crystallization had occurred. Even though the degree of crystallinity based on the calculations of the software for the samples studied were on average 22 %, this is not a true representation of the actual crystal content of the emulsion sample, where the solid content of the samples could be closer to 80 %. However, the purpose of the procedure was not to determine the absolute crystallinity of the material by PXRD, but rather to give an indication of the crystallization rate. Hence, by normalizing all preceding results to the one sample result that could be considered as having fully crystallized, one can then obtain an indication about the process of crystallization.

In this study, the crystallization rate comparison of the two emulsions made with different SMO concentrations is described using the Rietveld refinement rather than the peak intensity ratio approach in determining the degree of crystallization (Table 2).

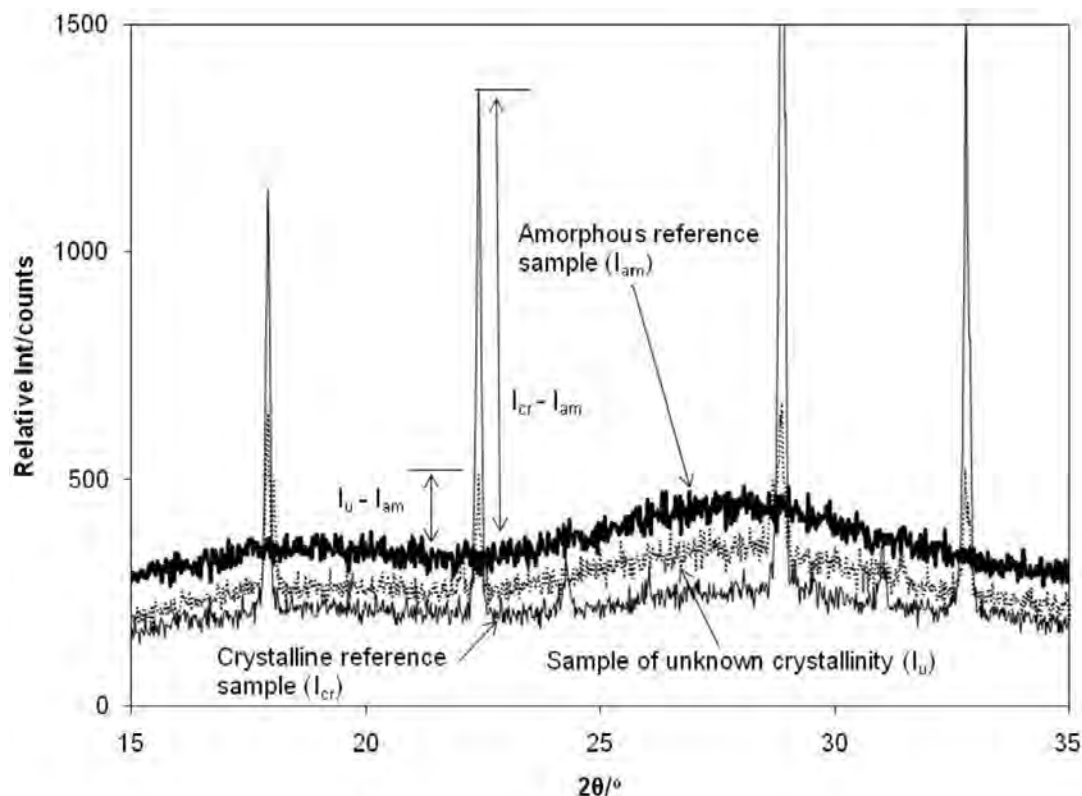


Figure 2 Diffraction patterns of a fully crystalline material, an amorphous material and a material of unknown crystallinity. Only the 2θ range from 15 to 35° is shown.

The crystallization process can be described by using the Johnson-Mehl-Avrami-Kolmogorov (JMAK) equation.

$$X_{CR} = 1 - e^{-\left(\frac{t}{\theta}\right)^n} \quad (3)$$

where X_{CR} is the degree of crystallization, t is time (days), θ is the characteristic time-related constant of the process and n an empirical factor called the Avrami exponent. The Avrami exponent is a useful parameter that can reflect the nucleation or growth characteristics during the crystallization process. It can give an indication of the geometry of crystal growth, where in a 3D-case, n has a maximum value of 4. In the case of a two dimensional (planar) type growth, n would be close to 3 where sporadic nucleation would be taking place.²² The linearized form of Equation 3 can be used to determine θ and the empirical factor (n)

from the slope and y -axis intercept.

$$\ln\left(\ln\frac{1}{1-X_{CR}}\right) = n\ln t - n\ln\theta \quad (4)$$

The values in Table 2 are normalized relative to the highest degree of crystallinity measured and used to determine the time constant and Avrami exponent. In the samples under investigation, an n value close to 3 was calculated from obtaining the best linear fit using Equation 4. The calculated results were then compared with the experimental values of X_{CR} using Equation 3 (Fig. 7).

The experimental results showed a reasonably good fit to the calculated equation with time constants (θ) of 42.6 and 54.2 days for the two samples made with 20 and 35 % SMO, respectively.

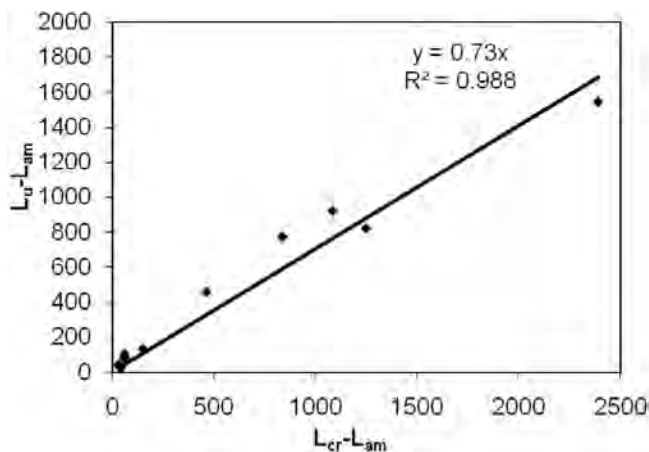


Figure 3 A plot of $(I_u - I_{am})$ versus $(I_{cr} - I_{am})$ for the eleven 2θ positions for a sample of unknown crystallinity. The slope of the straight line graph is equal to the relative crystallinity of the material.

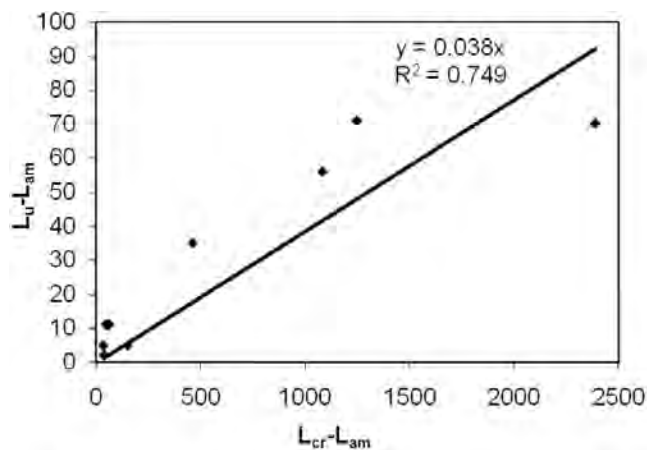


Figure 4 A plot of $(I_u - I_{am})$ versus $(I_{cr} - I_{am})$ for the eleven 2θ peak positions of a sample with relatively low crystallinity when compared with a fully crystallized sample. The slope of the straight line graph is equal to the relative crystallinity.

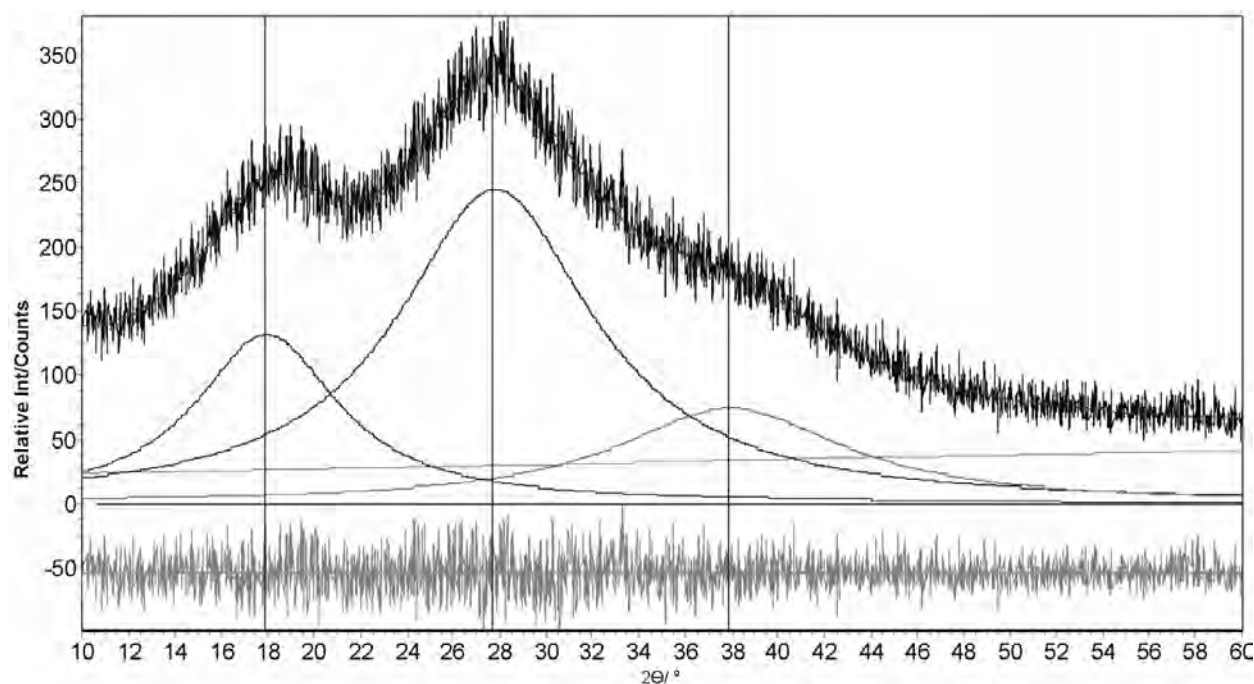


Figure 5 PXRD pattern of a newly-prepared AN emulsion showing the fitting of three broad peaks to describe the amorphous halo scattering.

Obtaining an Avrami exponent (n) close to 3 implied that the system corresponded to a sporadic type of nucleation process. Even though the process could be considered relatively slow (a few months), once the nucleation started, further crystallization proceeded quickly.²²

An interesting phenomenon was observed for some samples that underwent very slow crystallization, for example, the AN emulsion made with 20 % PIPSA. These showed the unusual appearance of the higher temperature AN phase II during the crystallization process, in addition to the room temperature phase IV (Fig. 8). This was observed during the Rietveld refinement analysis where there were unmatched peaks present that were not part of the typical phase IV pattern, but rather corresponded to phase II of AN. This was unusual as phase II of pure AN occurs only at temperatures above 84 °C or around 51 °C when there is sufficient moisture present (Table 1).

Hence, when determining the degree of crystallinity for these samples one has to consider the contribution of both phases IV and II of the crystalline part relative to the amorphous area. The ratio of phase IV to phase II changed with crystallization time, where the final fully crystallized sample was predominantly phase IV (Table 3). The Rietveld refinement method would take both crystal phases into consideration when determining the degree of crystallinity relative to the amorphous content.

The AN II phase would only be present during the initial crystallization, and with time changed to the AN phase IV, that can be considered to be thermodynamically more stable at room temperature. Even though the samples were kept at 22 °C, the slow kinetics of crystallization of the supersaturated solution would favour the formation of the high temperature phase II (Table 3). This was not observed in relatively faster crystallizing samples (those made with SMO), where phase IV was predominantly present. The explanation of this phenomenon could be in the sample preparation, where the solution of 80 % AN was at 80 °C. Once the hot saturated solution of AN was allowed to cool, under normal conditions, the AN phase II would be the solid phase that would start to crystallize at about 50 °C and go through the transitions to the room temperature phase IV. Since it was a supercooled emulsion at room temperature, the normal

Table 2 Change in relative crystallinity with time of the AN emulsions made with 20 and 35 % SMO.

Sample age/days	Relative crystallinity/%	
	20 % SMO	35 % SMO
0	0	0
18	1.49	1.1
20	2.6	–
27	4.37	0.8
39	15.6	5.1
47	16.4	14.8
59	21.1	20.3
72	21.6	23.4
94	20.7	22.6
117	–	22.7

solid-solid phase transitions did not occur. However, when the crystallization process of the emulsion seemed to occur significantly slower (after 90 days), the supercooled phase had a type of 'memory effect' in that the change would have to go firstly *via* AN phase II before proceeding to the room temperature phase IV. In part, the slow crystallization process could start by some 'seeding' sites in the emulsion droplet that still inherently had the solid AN phase II, where the nucleating ability to adjacent emulsion droplets could be impaired by a possible templating effect of the surfactants and hydrocarbon oil used. On the other hand, the faster crystallizing samples showed no such transitions when using PXRD analysis. This was also true for samples (not reported in this study) that had different PIPSA concentrations and hydrocarbon oils that showed relatively faster crystallization. These did not show the intermediate phase transition from phase II to IV. This could be explained either by the fact that the AN phase II to phase IV transition was relatively quicker for the faster crystallization samples where it could not be observed in time by PXRD, or that the supercooled solution would crystallize into phase IV only. At this stage, the exact mechanism of this observed phenomenon cannot be fully explained.

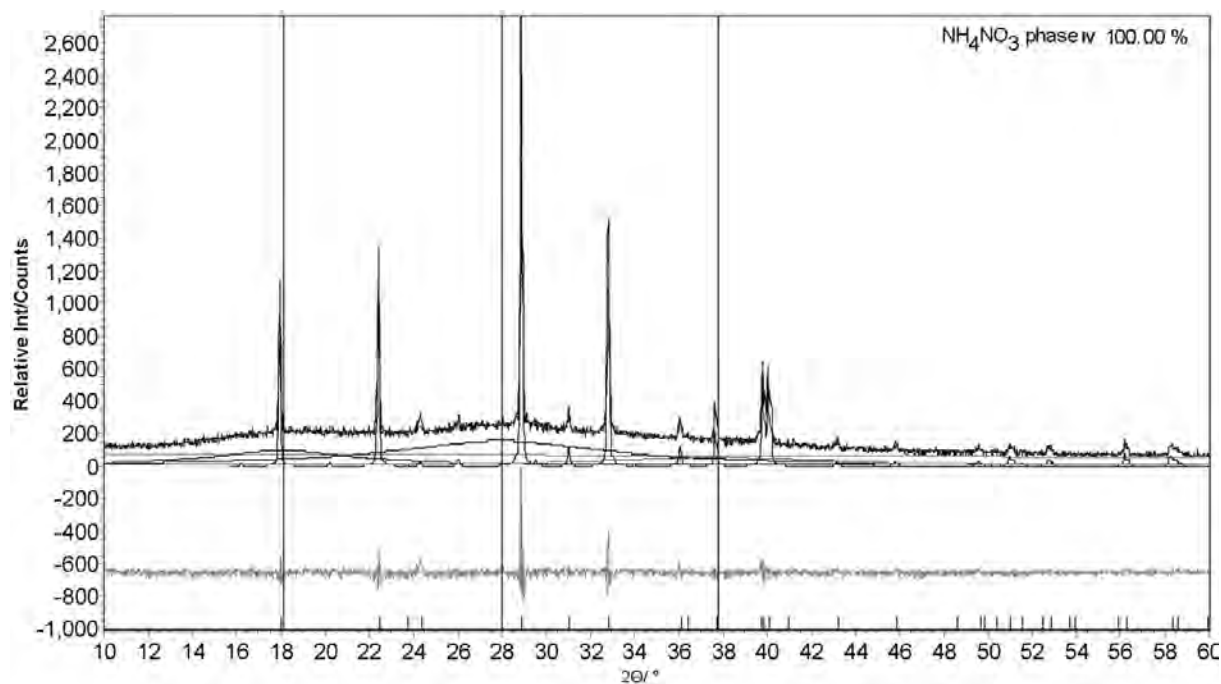


Figure 6 PXRD pattern of an aged AN emulsion showing complete crystallization with a degree of crystallinity of 21.7 %.

The results shown in Table 3 only report the ratio of phase IV to phase II for the samples above 1.2 % crystallinity. Results below this concentration are unreliable, since the peaks observed were very small, and only phase IV was considered in the degree of crystallinity calculations. Once the crystallization had proceeded, the two phases were clearly distinguishable from each other with good PXRD peak identification and solid phase composition by using the software's Rietveld refinement. A similar crystallization rate model to that of the previous set of results was used to show the change in crystallinity with time. The normalized crystallization comparisons considered both the AN phase IV and II as part of the total crystallization that had occurred (Fig. 9).

The results can also be described by using the JMAK equation where the Avrami exponent obtained was close to 3 with a time constant of 160.7 days.

3.2. The Influence of Temperature on the Crystallinity of AN Emulsions

Selected samples with various degrees of crystallinity were analyzed by VTPXRD. Samples that had achieved a high degree of crystallinity, when heated from 22 °C to 60 °C at 10 °C intervals, showed typical solid-solid phase transitions of AN phases IV to III to II (Fig. 10). This was similar to the solid-solid transitions observed for pure AN (Table 1), except that the phase transition

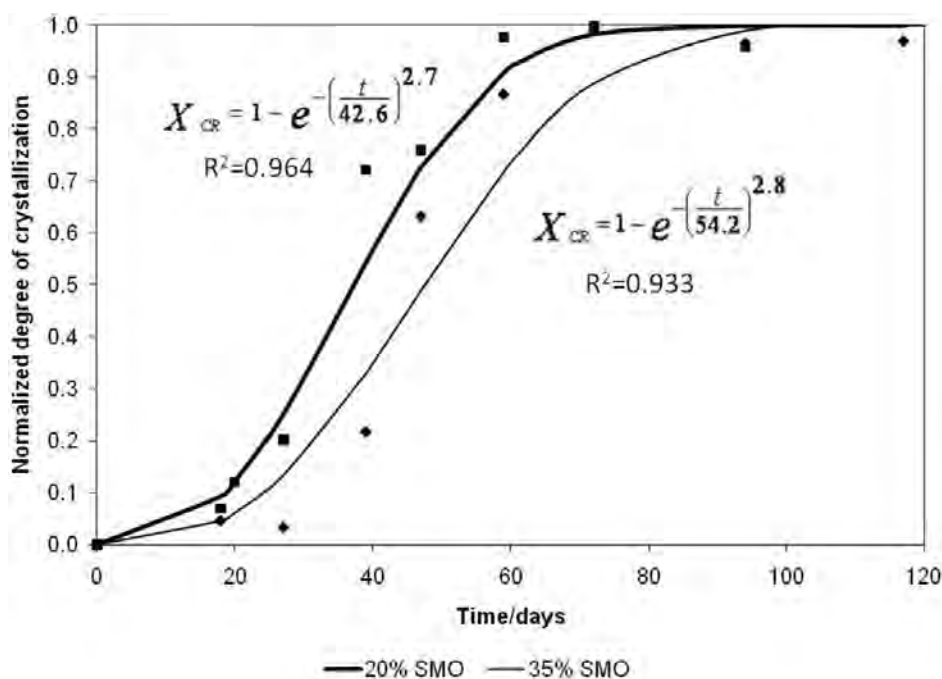


Figure 7 Plot of the experimental and derived crystallization results with time using the JMAK equation for AN emulsions made with 20 % and 35 % SMO, respectively.

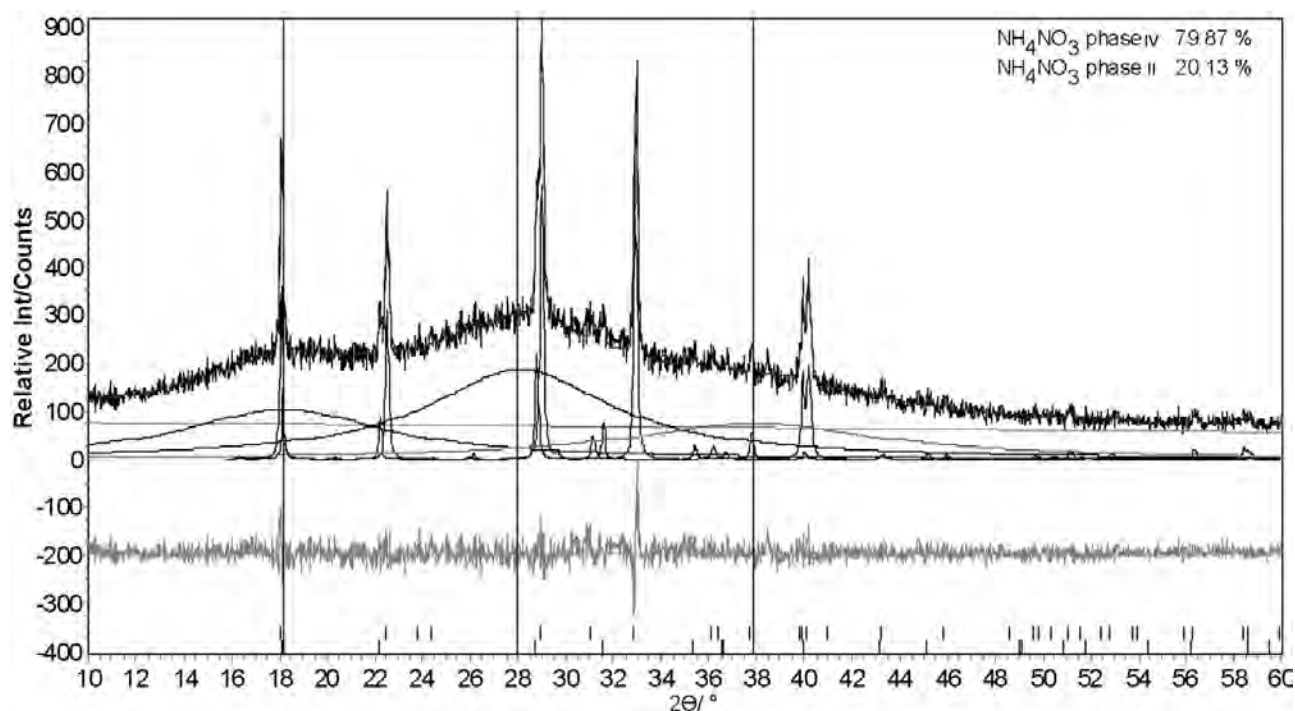


Figure 8 AN emulsion made with 20 % PIPSA that contained 79.87 % phase IV and 20.13 % phase II. The degree of crystallinity was 12.4 % with a Rwp of 8.31 and a GoF of 1.12.

from III to II was at a considerably lower temperature.¹⁵ The X-ray diffraction results showed that when a sample was allowed to cool from 40 °C to 22 °C, the expected transition from phase III to phase IV was observed. However, the diffraction pattern showed only a few peaks (Fig. 10). On cooling, the sample had undergone extreme texturing along certain crystal planes. In the example (Fig. 10), the X-ray diffraction pattern of the 22 °C sample after being heated to 40 °C showed very strong peaks at $2\theta = 22.5^\circ$ and 36° that corresponded to the (110) and (002) planes of AN phase IV.

In the VTPXRD analysis, a point detector (scintillation counter) was used by the diffractometer that was set up in a θ - θ configuration to measure along a one dimensional (1D) line only. An area detector on a 2D system would have shown such type of texturing by grainy or spotted diffraction rings. The property of texturing for AN material is not unusual, where the solid-solid phase transitions prefer to grow along certain preferred crystal

Table 3 Changes in relative crystallinity (%) with time (days) of the AN emulsion made with 20 % PIBSA. The changes in the relative mass (%) of AN phase IV to phase II with time are also shown.

Sample age/days	Relative crystallinity/%	AN Phase IV/%
0	0	–
18	0.1	–
27	0.2	–
39	0.4	–
59	0.6	–
72	1.2	–
94	2.2	28
117	4.8	57
133	7.3	80
170	16.3	96
186	21.7	100
188	20.4	100
214	22.3	100
249	23.2	100

planes when heated or cooled.¹⁶ Upon heating the sample again to 40 °C, typical crystalline peaks that corresponded to phase III were observed. On the other hand, AN samples that had a relatively low degree of crystallinity did not show the typical solid-solid phase transitions mentioned previously. Instead, they showed a solid-solid transition from phase IV to II above 50 °C (Fig. 11).¹⁵

The DSC analysis of the samples studied by the VTPXRD technique showed that a fully crystallized sample, on heating to 60 °C, indicated a number of solid-solid phase transitions (Fig. 12). The transition at 35 °C would correspond to the phase IV to phase III transition followed by the III to II transition at 44 °C (Fig. 12A). A smaller transition at 52 °C could correspond to a small amount of phase IV transforming to phase II typically seen for low crystallinity samples that show the IV to II transitions. Samples with a lower degree of crystallinity (1 %), showed a small transition at 52 °C, that could correspond to the typical phase transition of phase IV to phase II. Samples with 5 % crystallinity showed only two transitions close together at 43 and 46 °C, respectively (Fig. 12C). A possible problem with the reliability of the DSC results was that only small amounts of sample are used for analysis when compared with PXRD that give a more representative set of results over a larger sample area.

4. Conclusion

The technique of using PXRD with Rietveld whole-pattern refinement was shown to be a suitable method for determining the relative crystallinity of HCE AN samples. The software analysis could easily handle samples that had multiple solid phases present in the emulsion mixture with strong preferred orientation. These factors could easily be accommodated in the analysis to obtain a comparative degree of crystallinity in order to determine the rate of crystallization.

The JMAK kinetic model was used to describe the rate behaviour of the crystallization process with time where the Avrami exponent close to 3 indicated a sporadic type of crystallization

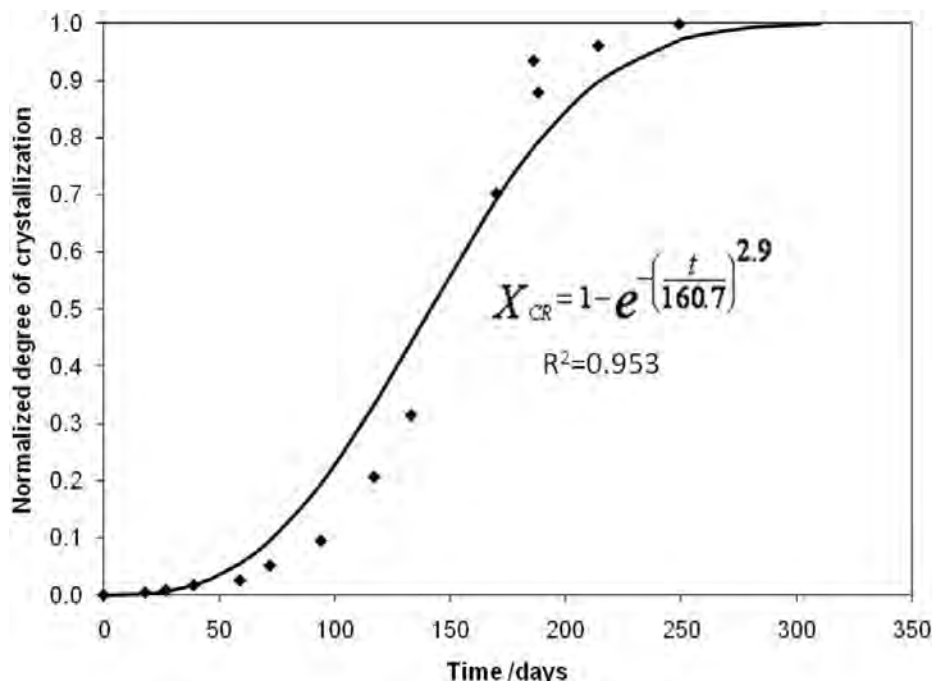


Figure 9 Plot of the experimental and derived crystallization results with time using the JMAK equation for AN made with 20 % PIBSA

process, even though the relative time for complete crystallization to occur in some samples was more than 250 days.

Samples that underwent relatively slow crystallization showed that the initial crystallites formed were of the higher temperature AN phase II before changing to the more stable room temperature phase IV with time. This implied a type of structural 'memory effect' of the supercooled emulsion that

could have originated from the heated solution during sample preparation.

Partially crystallized AN emulsions can be heated to 60 °C without losing their emulsion properties and showed the typical solid phase IV to phase II transition. Emulsions that had a higher degree of crystallinity or those that were fully crystallized would undergo the IV to III to II transition upon heating. A consider-

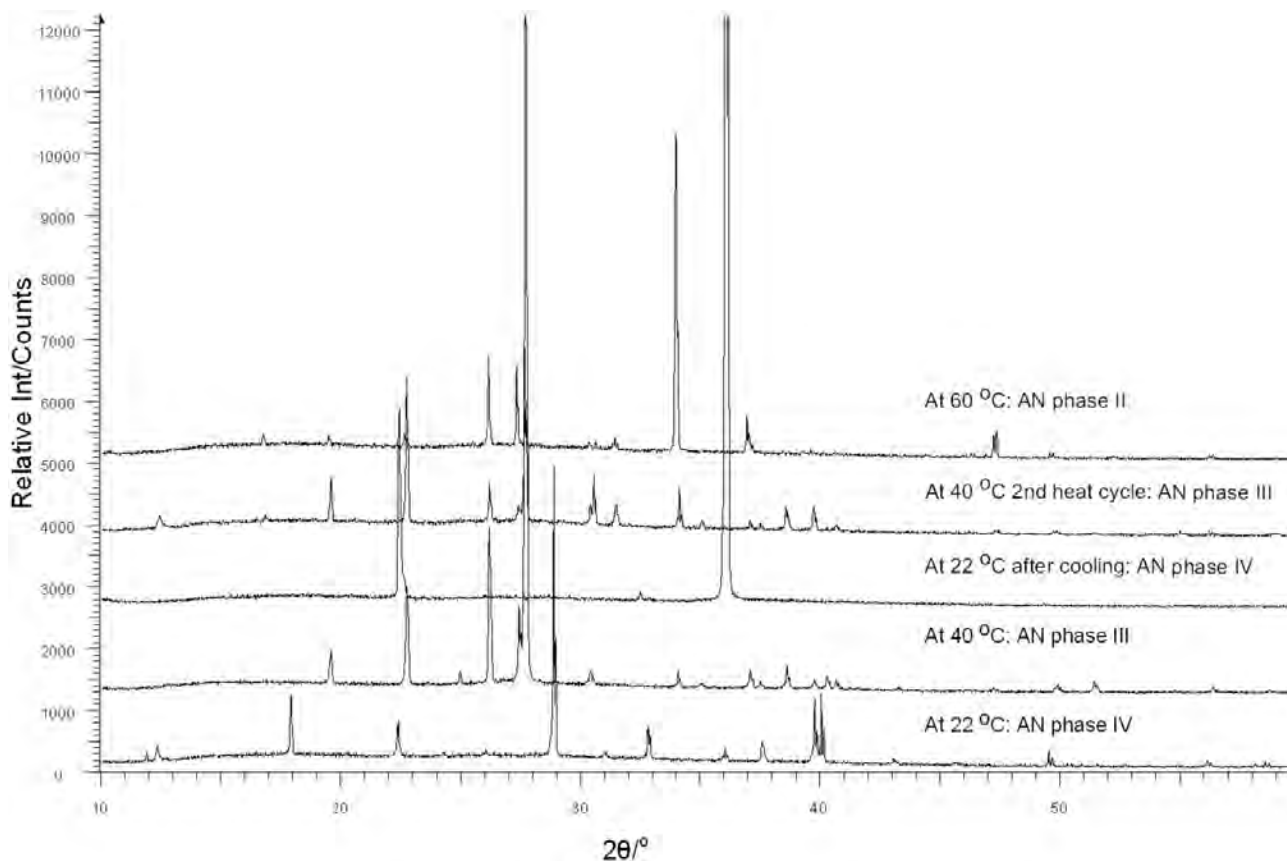


Figure 10 VTPXRD patterns of various samples that were heated and cooled of a fully crystallized AN emulsion (22 %) made with 35 % SMO. The diffraction pattern of the sample was done at 22 °C, at 40 °C followed by cooling to 22 °C, then heating to 40 °C again and then to 60 °C.

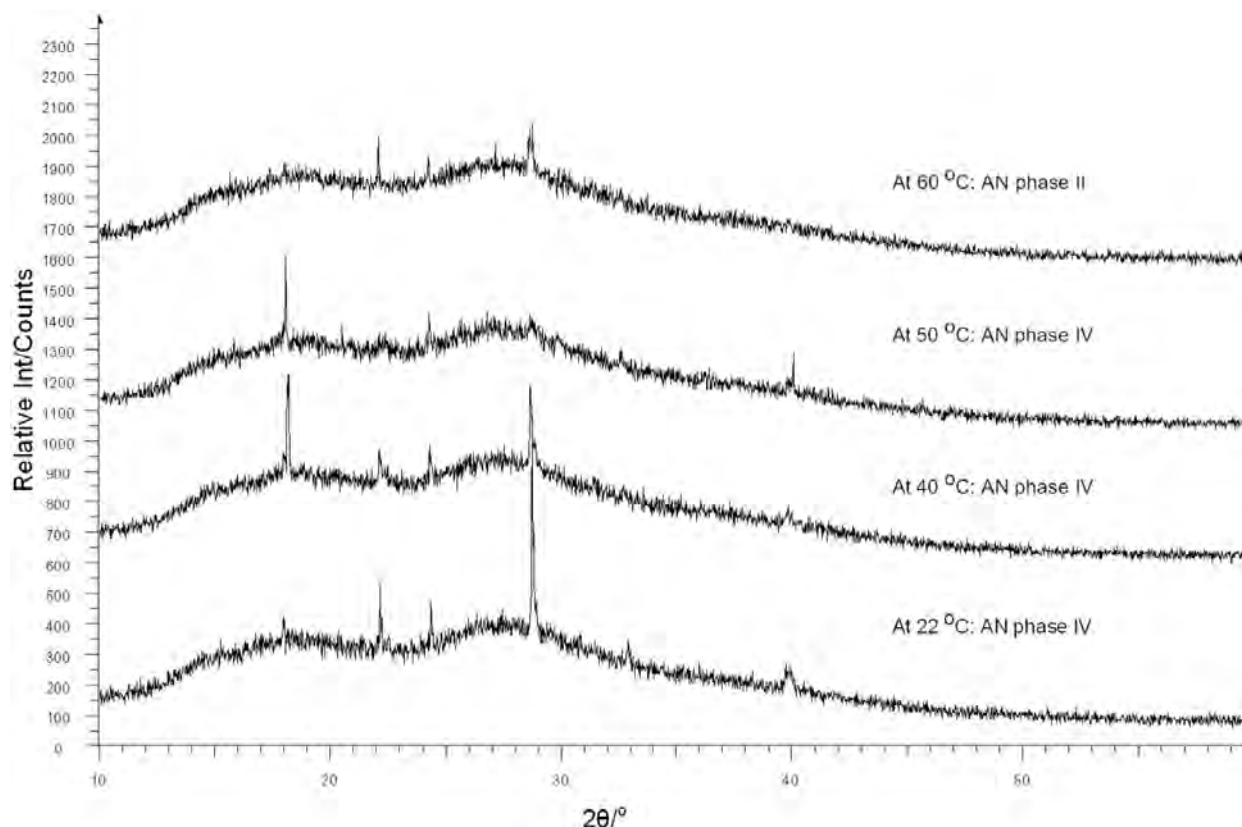


Figure 11 VTPXRD patterns of an AN emulsion made with 35 % PIPSA that had only 2.5 % relative crystallinity. The diffraction patterns of the sample were done at room temperature, 40 °C, 50 °C and 60 °C.

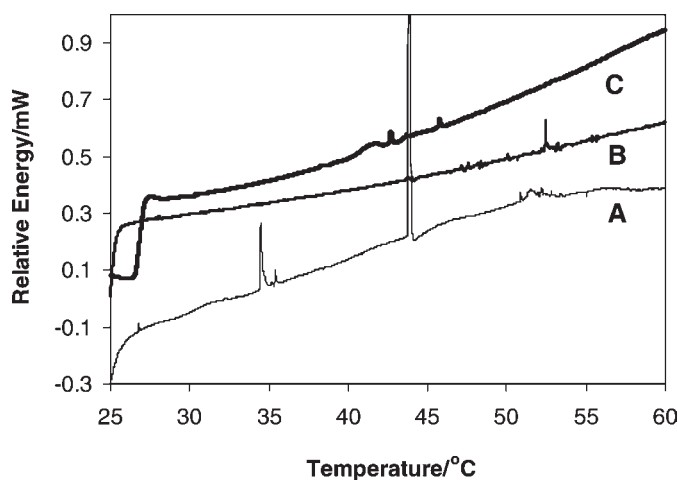


Figure 12 DSC heating curves of various crystallized AN samples showing a number of solid-solid phase transitions. A: 21 % crystallized; B: 1 % crystallized and C: 5 % crystallized.

able amount of texturing along certain crystal planes was also observed in samples upon cooling when changing from one solid phase to another.

Acknowledgements

The authors thank the South African National Research Foundation (NRF) for funding towards the project.

References

- H.A. Bampfield and J. Cooper, *Emulsion Explosives*, in *Encyclopaedia of Emulsion Technology*, Marcel Dekker, New York, NY, USA, 1985.
- R. Pons, C. Solans, M.J. Stebe, P. Erra and J.C. Ravey, *Prog. Colloid Polym. Sci.*, 1992, **89**, 110–113.

- I. Masalova, A.Y. Malkin, E. Ferg, E. Kharatiyan, M. Taylor and R. Haldenwang, *J. Rheology*, 2006, **50**, 435–451.
- I. Masalova, A.Y. Malkin, P. Slatter and K. Wilson, *J. Non-Newtonian Fluid Mech.*, 2003, **112**, 101–114.
- F. Villamagna and M.A. Whitehead, *J. Mol. Struct.*, 1995, **356**, 149–158.
- P. Bergese, I. Colombo, D. Gervasoni and L.E. Depero, *J. Appl. Cryst.*, 2003, **36**, 74–79.
- M. Kakudo and N. Kasai, *X-ray Diffraction by Polymers*, Kodansha Scientific Books, Tokyo, Japan, 1972.
- R. Surana and R. Suryanarayanan, *Powder Diff.*, 2000, **15**, 2–6.
- S. Yamamura, R. Takahira and Y. Momose, *Pharm. Res.*, 2007, **24**, 880–887.
- X. Chen, S. Bates and K.R. Morris, *J. Pharm. Biomed. Anal.*, 2001, **26**, 63–72.
- N.G. Parsonage and L.A.K. Staveley, *Disorder in Crystals*, Oxford University Press, Oxford, UK, 1978.
- A. Guinier, *X-ray Diffraction in Crystals, Imperfect Crystals and Amorphous Bodies*, Dover Publications, New York, NY, USA, 1994.
- P. Suortti, *J. Appl. Cryst.*, 1972, **5**, 325–331.
- A. Coelho, *J. Appl. Cryst.*, 2000, **33**, 899–908.
- E. Ferg, D.C. Levendis and F.R.L. Schoening, *Chem. Mater.*, 1993, **5**, 1293–1298.
- J.C.A. Boeyens, E. Ferg, D.C. Levendis and F.R.L. Schöning, *S. Afr. J. Chem.*, 1991, **44**, 42–46.
- C.S. Choi, H.J. Prask and E. Prince, *J. Appl. Cryst.*, 1980, **13**, 403–409.
- ICDD, International Centre for Diffraction Data, Philadelphia, PA, USA, 2004.
- I. Masalova and A.Y. Malkin, *Colloid J.*, 2007, **69**, 198–201.
- Bruker AXS, *Topas V3: General Profile and Structure Analysis Software for Powder Diffraction Data*, Bruker AXS, Karlsruhe, Germany, 2005.
- P. Stutzmann, *Adv. X-ray Anal.*, 2004, **47**, 206–211.
- L. Mandelkern, *Crystallization of Polymers*, McGraw-Hill, New York, NY, USA, 1964.